Article

Not peer-reviewed version

Multifaceted Applications of Silver Nanoparticles Synthesized from Marine Fungus *Aspergillus flavus* MK4: Antimicrobial, Anticancer, and Wound-Healing Properties

Mohamed H Al-Agamy [*] , Mahmoud S Kelany , Wael A Mahdi , Sultan Alshehri , Mohammad R Alhuzani , Moaz M Hamed

Posted Date: 26 December 2023

doi: 10.20944/preprints202312.1737.v1

Keywords: Biosynthesis; silver nanoparticle; marine fungi; antimicrobial activity; antioxidant activity; cytotoxic activity

Article

Multifaceted Applications of Silver Nanoparticles Synthesized from Marine Fungus *Aspergillus flavus* MK4: Antimicrobial, Anticancer, and Wound-Healing Properties

Mohamed H. Al-Agamy [1,2,3]*, Mahmoud S. Kelany [4], Wael A. Mahdi [1], Sultan Alshehri [1], Mohammad R. Alhuzani [2] and Moaz M Hamed [4]

[1] Department of Pharmaceutics, College of Pharmacy, King Saud University, 11451 Riyadh 2457, Saudi Arabia
[2] Microbiology Unit, Central Lab, College of Pharmacy Research Center, King Saud University, 11451 Riyadh 2457, Saudi Arabia
[3] Department of Microbiology and Immunology, Faculty of Pharmacy, Al-Azhar University, Cairo, Egypt
[4] National Institute of Oceanography and Fisheries (NIOF), Egypt.

Abstract: Due to their wide range of uses in modern technology, nanomaterial's of silver metallic (Ag-NPs) have engaged considerable concern, driving significant research with development efforts. This study focuses on investigating the antimicrobial properties of Ag-NPs, encompassing their production, characterization, and biological aspects. The eco-friendly extracellular biosynthetic method employed in this work utilized extracts from the marine fungus *Aspergillus flavus* MK4 as reducing agents for nanoparticle synthesis. Analyzing the colloidal Ag-NPs using UV-visible spectroscopy revealed a peak in absorbance at 460 nm, indicating the presence of plasmonic properties. The electrons imaging of internal structure (TEM) elucidated spherical shape of the Ag-NPs by 15 nm size. Testing against bacterial diversities (Gr-ve & Gr+ve) revealed potent antibacterial and antifungal efficacy. Cytotoxicity versus HepG-2 cell line was assessed using the MTT assay, and antioxidant properties were examined through the radical scavenging (DPPH) assay. In wise of their conceivable applications in the fields of antibacterial, anticancer, and wound-healing, the Ag-NPs that were synthesized exhibit promising features. With its powerful ability to synthesize silver nanoparticles (Ag-NP), *Aspergillus flavus* MK4 Aspergillus flavus MK4 can generate nanoparticles extensively characterized, demonstrating their antibacterial, antioxidant, anticancer, and wound-healing properties.

Keywords: biosynthesis; silver nanoparticle; marine fungi; antimicrobial activity; antioxidant activity; cytotoxic activity

1. Introduction

The term "marine fungi" encompasses a diverse range of fungi typically inhabiting natural environments within marine and estuarine settings [1]. Fungi that live in marine environments can be found in a wide variety of habitats within each marine ecosystem. The fact that they develop crucial symbiotic connections with other species, such as algae and sponges, gives them significance that goes beyond their mere presence. Marine fungus are crucial in the process of recycling nutrients and decomposing carbon-based compounds with playing a powerful role in the maintenance of healthy marine ecosystems and the proper functioning of marine ecosystems [2].

Ascomycota, Basidiomycota, and Chytridiomycota are the three basic phyla that are considered to be included of the realm of marine fungi that is being studied by science. These fungi can be found in a broad range of marine ecosystems, spanning from the open ocean to sediments, mangroves, and coral reefs. Their distribution is highly diverse, encompassing all of these environments. Notably, several marine mushrooms have shown that they are able to thrive even in the darkest parts of the ocean, where there is very little light. It is because of this versatility that marine fungus are able to occupy a wide variety of ecological niches across settings that are marine [3]. Numerous marine

 doi:10.20944/preprints202312.1737.v1

fungus has developed special adaptations that allow them to flourish in settings that are submerged in water. The osmoregulatory systems that these fungi have developed allow them to maintain the stability of their internal salt concentrations despite the fact that the surrounding conditions are constantly changing. In addition to this, they are capable of producing secondary metabolites, such as polyketides and terpenoids, which possess antibacterial, antiviral, and antifungal effects. The ability of marine mushrooms to traverse and respond to the challenges given by their aquatic habitats is highlighted by these adaptations, which contribute to the marine fungi's ability to survive and play ecological functions within the marine ecosystem [4].

There is no doubt that nanotechnology stands out as one of the technologies that is extremely promising and is progressing at a rapid pace. The synthesis of nanoparticles, which are materials with unique features that are achieved by reducing bigger substances to the atomic scale, is the fundamental activity that underpins this discipline. Nanoparticles are endowed with amazing capabilities due to their size range, which ranges from one to one hundred nanometers. Their high surface area to volume ratio, stemming from their compact structure, facilitates significant interactions and enhances responsiveness. In addition, the fact that they are so small makes it simple to modify their surface qualities, which enables them to be tailored to specific applications using the properties. All of these characteristics, taken together, lead to the extraordinary adaptability of nanoparticles and the potential uses they have in a wide range of scientific, industrial, and medical domains [5]. Silver nanoparticles (Ag-NPs) have attracted significant attention owing to their distinctive physicochemical characteristics and diverse applications in fields such as medicine, electronics, and environmental remediation. The appeal of marine fungi lies in their potential to serve as a bioactive chemical source, making them especially attractive for synthesizing (Ag-NPs). The combination of marine fungi and silver nanoparticles presents a substantial opportunity to improve the production of these nanoparticles, potentially leading to unique features and a wide range of applications in various fields [6]. A wide range of industries, including agriculture, commerce, medical, and manufacturing, are already making extensive use of silver nanoparticles through their ubiquitous application. Because of their diverse qualities, they can be applied across a range of sectors and in various applications [7]. Silver nanoparticles (Ag-NPs) have diverse applications in medicine, serving as enhancers for vaccinations, drugs for diabetes, agents for wound and bone healing, components in biosensors, and contributors to anticancer treatment. The unique features of Ag-NPs emphasize their importance in medical applications, emphasizing the prospective role they play in advancing healthcare and medical interventions [8]. Marine fungi facilitate the biosynthetic process that transforms silver ions (Ag+) into elemental silver (Ag) through the generation of silver nanoparticles (Ag-NPs). Enzymes and/or metabolites produced by the fungi play a crucial role in aiding this conversion. Although the entire mechanism of Ag-NP biosynthesis remains incompletely understood, it is thought to entail the reduction of Ag+ to Ag0. The synthesis of silver nanoparticles (Ag-NPs) entails the involvement of enzymes like reductases and nitrate reductases, along with secondary metabolites such as terpenoids, flavonoids, and phenolic compounds. These components collectively contribute to the reduction process, and their intricate interplay is believed to be pivotal in producing silver nanoparticles with distinct and precise characteristics. [8-10].

Several marine fungi, including *Aspergillus, Penicillium, Fusarium*, and *Trichoderma*, have been identified as capable of biosynthesizing (Ag-NPs). Researchers have employed various characterization methods to analyze these biosynthesized Ag-NPs. Several methods, such as UV-vis spectroscopy, transmission electron microscopy (TEM), X-ray diffraction (XRD), and Fourier-transform infrared spectroscopy (FTIR), are employed to gain valuable insights into the physical, chemical, and structural characteristics of the silver nanoparticles (Ag-NPs) generated by marine fungi [9]. The advantages of employing marine fungi in the biosynthesis of Ag-NPs, in contrast to chemical and physical approaches, include utilizing renewable resources, minimizing energy consumption, and enabling the potential for widespread production on a large scale. Moreover, the Ag-NPs produced by the process of biosynthesis by marine fungi have exhibited potent antibacterial, antioxidant, and anticancer properties. This renders them highly appealing for many medical applications [11].

 doi:10.20944/preprints202312.1737.v1

Our aim in this research is to synthesize (Ag-NPs) utilizing the cell-free filtrate (CFF) derived from the marine fungus *Aspergillus flavus*. he morphological and structural features of the generated nanoparticles were extensively analyzed using methods such as UV-vis spectroscopy, TEM imaging, FTIR, and XRD. The antibacterial effectiveness of Ag-NPs was investigated after synthesis by exposing them to different pathogenic bacteria. The antioxidant properties of Ag-NPs were assessed through the DPPH assay. Additionally, the cytotoxicity of the silver nanoparticles was examined.

2. Material and Methods

2.1. Tested bacterial isolates which used in antimicrobial test

Bacillus subtilis ATCC 6633, *Staphylococcus aureus* ATCC 25923, and *Bacillus cereus* are examples of Gr+ve strains. Additionally, there are Gr-ve strains, including *Pseudomonas aeruginosa* ATCC 9027, *Salmonella typhimurium* ATCC 14028, *Pseudomonas fluorescens* DSM 50090, and *Aeromonas hydrophila* NRRL 914.

Tested fungal isolates which used in antifungal test

The fungal strains NIOF-F3, NIOF-F8, NIOF-F12, NIOF-F13, NIOF-F15, NIOF-F22, NIOF-F48, NIOF-F63 and NIOF-F71, which namely *Aspergillus fumigatus*, *Aspergillus niger*, *Aspergillus flavus*, *Aspergillus terreus*, *Aspergillus parasiticus*, *Penicillium oxalicum*, *Fusarium solani*, *Fusarium oxysporum* and Candida albicans [12], were sourced from the NIOF Microbiological Lab at the NIOF, Red Sea branch in Egypt. These marine pathogenic strains were maintained on YPD agar slants (yeast extract peptone dextrose) and preserved for an extended period at approximately 4 °C by folding the slants with 25% glycerol.

2.2. Sampling and fungal isolation

Aseptic procedures were utilized to gather sediment samples from various locations, including the Suez Gulf, Hurghada city, the National Institute and Oceanography Beach. The specific coordinates for these locations are 27° 17' 03" N latitude and 33° 46' 15" E longitude. The sampling focused on the plow layer, spanning depths from 0 to 25 cm. Each sediment sample, weighing approximately 100g, was meticulously deposited into sterile vials, each appropriately labeled [13]. Fungi isolation involved employing the serial dilution technique. Initially, a gram of sediment sample was suspended in 10 ml of sterile seawater, resulting in the generation of serial dilutions ranging from 10^{-1} to 10^{-5}. The next step was to inoculate modified Potato Dextrose Agar (MPDA) media (containing potatoes (sliced washed unpeeled), 4 g (from 200 g infused potato); dextrose, 20 g; di-potassium hydrogen phosphate, 1.0; potassium nitrate, 2.0; magnesium sulphate, 0.5; agar, 18.0 and distilled water, 1 L with 1 % streptomycin) with 1 mL of each dilution. After inoculation, the medium-petri dishes were transferred to an incubator set at a temp. of 28 ± 2 °C, where they were allowed to remain undisturbed for a duration of 14 days. Throughout the week-long observation period, the fungal colonies were carefully monitored. Pure cultures of the observed fungal colonies were identified and maintained for further analysis [14].

2.3. Preparation of cell-free extract

To create the inoculum for the fungal broth, a loop carrying approximately 1 × 10^6 spores of selected isolates was transferred into 50 mL of Modified Potato Dextrose (MPD) broth media. The transfer was executed using a 250 ml Erlenmeyer flask. To synthesize (Ag-NPs), a fungal inoculum was introduced into a 250 mL conical flask filled with MPD broth. The flask underwent incubation on a rotary shaker at 220 rpm for five days at a temperature of 28 ± 2 °C. Following that, the culture was subjected to centrifugation at 10,000 rpm to gather the supernatant, a critical component necessary for the synthesis of (Ag-NPs) [15].

2.4. Green synthesis of Ag-NPs

The supernatants, also referred to as biomass filtrate, were engaged to synthesis of eco-friendly Ag-NPs. In 100 ml Erlenmeyer flasks, 30 mill of 10 mill mole $AgNO_3$ was combined with 90 ml of isolated supernatant. The incubation of the flasks was carried out at 28 ± 2°C, and observations were

 doi:10.20944/preprints202312.1737.v1

made for any color changes. Two controls were implemented for comparison: In the initial control, sterile media was blended with 10 mM silver nitrate, this control served to validate that the media components alone were incapable of silver ions transformation to nanomaterial's containing silver. In the negative control, which consisted of a silver nitrate solution, no observable color change occurred over time. Daily monitoring of the flasks was conducted to detect any visual alterations in color. Additionally, UV-visible spectroscopy, spanning the range of 200–800 nm, was performed for flasks displaying noticeable color adjustments. This analytical approach provides a detailed examination of the spectral characteristics associated with the synthesis of silver nanoparticles [16].

2.5. Characterizations of Ag-NPs

We utilized a METASHUV-9000A UV–Visible double-beam spectrophotometer to analyze the absorption spectra of the generated silver nanoparticles (Ag-NPs) over the wavelength range from 200 nm to 800 nm. To assess the morphology and dimensions of the synthesized Ag-NPs, Transmission Electron Microscopy (TEM) and Scanning Electron Microscopy (SEM) were employed. Fourier Transform Infrared Spectroscopy (FTIR) with the corresponding instrument was utilized to investigate the surface chemistry of the specimen (Nicolet 6700, Thermo Fisher Scientific). Moreover, an X-ray diffractometer was utilized to generate an XRD pattern of silver nanoparticles. The spectrum was recorded with CuKα radiation (wavelength: 1.5406 nm) within the 2θ range from 0^0 to 90^0, operating at 30 kV and 100 mA. [17].

2.6. Genotypic characterization of a potent isolate

The genomic DNA extraction from the isolated (MK4) utilized the cellular DNAeasy Kit, following the standard instructions. For the fungi, genomic DNA extraction was performed from cultures with seven day old using the DNeasy technologies provided by QIAGEN. The amplification of the ribosomal spacer DNA (ITS) was carried out using primers ITS1 and ITS4. Subsequently, purification of the PCR products was accomplished using the QIAquick kit [18]. The resulting PCR products were sent to Color Lab., Cairo, for sequencing. The obtained sequences underwent a BLAST search in GenBank (NCBI) for comparison with other relevant sequences.

Antimicrobial activity of Ag-NPs

The well diffusion method was employed to assess the antibacterial activity of the synthesized silver nanoparticles [19]. For all test bacterial strains, an overnight growth at 37°C in nutrient broth with a McFarland 0.5 adjustment was employed. Subsequently, 100µl from the tested isolates were aseptically spread on individual nutrient agar plates. Using a cork borer, a well with an 8 mm diameter was created on the agar plate, and 60µl of the synthesized Ag-NPs were introduced into each well under sterile conditions. Furthermore, a positive control was established with 100 µl of ampicillin (1 mg/ml), while negative controls comprised 60 µl each of 1 mM silver nitrate and culture broth (culture without $AgNO_3$). Afterward, the plates underwent a 24-hour incubation at 37°C, and the assessment of antibacterial activity involved measuring the diameter of the inhibition zone using a zone scale [17].

2.7. Anti-fungal test activity of Ag-NPs

The fungi inhibition efficacy of Ag-NPs was assessed through diffusion assay against the aforementioned fungal strains that's were enumerated by YPD medium with let them incubate for a duration of 3-5 days at 30 °C [20]. A suspension of fungi was prepared in a sterilized phosphate buffer solution (PBS) with a pH of 7.0. The inoculum was adjusted to a concentration of 10^6 spores/mL after being counted in a cell counter chamber. Wells measuring 8 mm in diameter were created using a sterile cork-borer. Subsequently, 60 µl of both Ag-NPs and $AgNO_3$ were separately introduced into each well and allowed to incubate for 2 hours at 4 °C. Nystatin was utilized as the reference antifungal agent, and the plates were subsequently incubated for a time of 3 days at 30 °C. Following the reproduction, the measurement and recording of inhibition zones were carried out [21].

2.8. Determination of antioxidant activity

 doi:10.20944/preprints202312.1737.v1

The radical scavenging activity of Ag-NPs and vitamin C was assessed using the DPPH (1-diphenyl-2-picrylhydrazyl) assay. Initially, 1 ml of Ag-NPs at various concentrations (10, 20, 30, 40, 50, 60, and 100 µg/ml) were mixed with 1 ml of 1 mM DPPH solution and vortexed. The mixture was then left undisturbed for 30 minutes at room temperature and in the dark. Subsequently, the absorbance was measured at a wavelength of 517 nm using the JENWAY 6800 Spectrophotometer. DPPH served as the control, while methanol was used as the blank [10]. The percentage of inhibition of free radical scavenging activity was estimated using the formula: **% of scavenging =[(Pc-Ps)] ×100** where Pc is the absorbance of the control and Ps is the absorption of Ag-NPs/vitamin C.

2.9. Cytotoxic Activity

After a 24-hour growth period at 37°C with 5% CO2, the hepatocellular carcinoma cell line was introduced into flasks containing Dulbecco's Modified Eagle's Medium (DMEM) enriched with 10% fetal bovine serum (FBS). Post-incubation, cells were trypsinized for 3-5 minutes at 800 rpm for 10 minutes to facilitate separation. For the experiment, a total of 96 wells in an ELISA plate were utilized, with 5,000 cells in each well. The cells were allowed to grow into a monolayer, reaching a confluence of 70-80% during a 24-hour incubation at 37°C. The toxicity of Ag-NPs was tested at concentrations ranging from 10 to 50 µg/ml in triplicates, and cell counting was performed under an optical microscope after 48 hours to assess viability. cytotoxicity solution was introduced into the culture medium for assessing cell viability. Each well was treated with 200 µl of MTT solution and then incubated for 4–5 hours. Following the removal of the MTT solution, 200 µl of DMSO was applied to each well in the absence of light for the subsequent incubation period. The optical density of the formazan product at 595 nm was determined using an ELISA reader from Biorad, USA [22].

2.10. Wound Healing Assay

The cell scratch assay was used to evaluate the wound-healing potential of silver nanoparticles in relation to the normal 3T3 fibroblast cell line. The experiment involved seeding 2×105 cells/ml in a combination of M199 medium and DMEM with 10% phosphate buffer saline (PBS). Following cell seeding, the samples were placed in a CO_2 incubator for 22-28 hours. Once a monolayer confluence of approximately 70–80% was achieved, the cells were scraped at the center of the culture well using sharp points. The damaged cells were then washed away with multiple fresh batches of media. Subsequently, the scratched wells were treated with the test samples (silver nanoparticles). The negative control was Hanks' Balanced Salt solution (HBSS), while the positive control was Allantoin, a commercial wound healing drug from Sigma Aldrich at a concentration of 50 µg/ml. After removing the plates from the incubator, they were further incubated for 22–24 hours to allow proper development. Phase-contrast microscopy images, documenting the wound healing activity, were captured after fixing and staining the cells [23].

2.11. Statistical analysis

Statistical analysis was performed using IBM SPSS Statistics 23. The experimental results were presented as means with standard errors (± SE). Following the one-way ANOVA analysis, the significance level was reported.

3. Results

3.1. Fungal isolation and screening for silver nanoparticle synthesis

The primary emphasis of the current study centered on the extracellular synthesis of (Ag-NPs) using the supernatant of marine fungi. Out of the twenty-three fungal isolates obtained from the sediment sample, their potential to generate silver nanoparticles was systematically evaluated. The screening process pinpointed a singular isolate, named MK4, which exhibited the capability for Ag-NP synthesis. Remarkably, the reduction of Ag^+ ions was visibly evident upon the addition of $AgNO_3$ to the supernatant of marine fungi, leading to a distinct color change from yellow to dark brown. In the control group, no such alteration in color was observed (see Figure 1). This highlighted the specificity and effectiveness of the Ag-NP synthesis process by the **MK4** isolate.

Preprints (www.preprints.org) | NOT PEER-REVIEWED | Posted: 26 December 2023 doi:10.20944/preprints202312.1737.v1

3.2. Analysis by UV-Visible spectroscopy

A UV-Visible spectrophotometer was used to verify the existence of metal nanoparticles (see Figure 1). A wavelength peak at 460 nm was seen in the spectra of silver nanoparticles. The fact that metal nanoparticles ranging in size from 2 to 85 nm usually show peaks when examined with UV-Vis spectrophotometers is widely known. The presence of this particular peak at 460 nm lends credence to the idea that silver nanoparticles were successfully synthesized in this study.

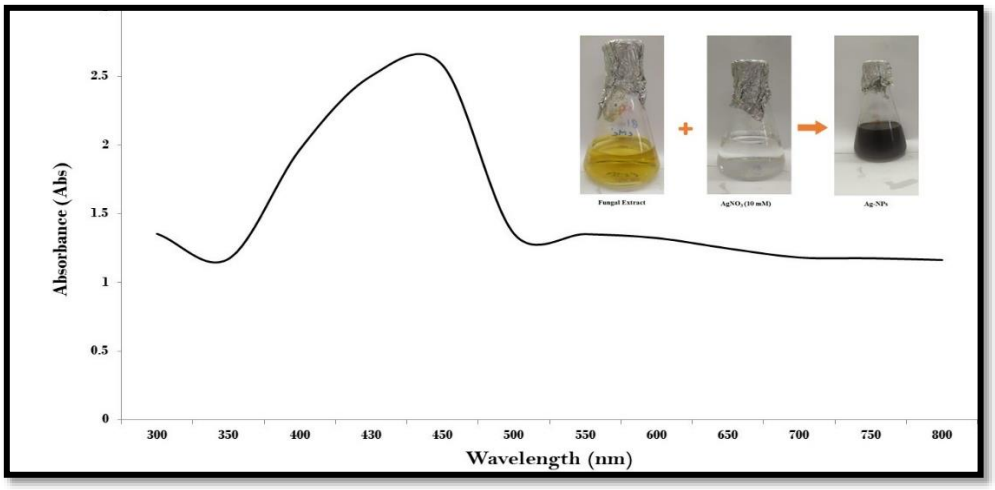

Figure 1. The fungal isolate (MK4) generated silver nanoparticles, as determined by UV-vis absorption spectra.

3.3. Fourier transform infrared spectroscopy

Absorbance bands arranged between 400 cm-1 and 4000 cm-1 were shown by the FTIR spectrum analysis. Figure 2 shows that the silver nanoparticles made from the marine fungus MK4 showed different bands. For Ag-NPs, the FTIR spectra revealed prominent absorption bands at 3417.58, 2921.14, 1631.68, 1553.49, 1452.97, 1383.59, and 1023.85 cm-1. A strong and wide absorbance peak at 3417.58 cm-1, which is the N-H stretch, suggests the presence of amines. The strong medium absorbance peak at 2921.14 cm^{-1} (C–H stretch) is associated with the alkanes group. The band at 1631.68 cm^{-1} (N–H bend) represents the characteristic feature of the amine group. The intense medium absorbance at 1553.49 cm^{-1} (N–O stretching) is characteristic of nitro compounds. The alkanes group is assigned to the band at 1452.97 cm-1, which is C-H bending. The presence of the 1383.59 cm-1 band suggests that the (C-N) vibrations are in a bending mode. As an added bonus, the stretching vibration of the carbon-oxygen bond is responsible for the bands observed at 1023.85 cm-1 in the FTIR spectra.

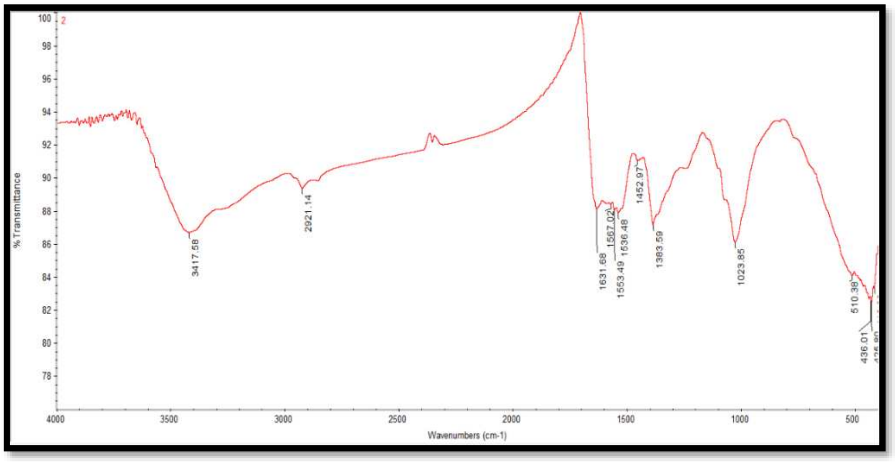

 doi:10.20944/preprints202312.1737.v1

Figure 2. The FTIR spectra of silver nanoparticles produced by the MK4 fungal isolate.

3.4. X-ray diffraction analysis

To find out if Ag-NPs were crystalline, X-ray diffraction (XRD) was used. This study focused on analyzing the XRD patterns of lyophilized Ag-NPs with the fungal isolate MK4, as seen in Figure 3. Six distinct diffraction peaks were seen at 2θ values of 28.8°, 32.7°, 37.9°, 45.0°, 55.4°, and 58.4°. Bragg reflections of metallic (Ag-NPs) formed in a face-centered cubic (FCC) structure are completely matched by the different peaks seen in the XRD pattern. These peaks correspond to specific lattice planes within the Ag-NP crystal, including the (111), (200), (024), (311), (116), and (222) planes (Figure 2). This remarkable agreement provides strong evidence for the successful synthesis of crystalline Ag-NPs with a well-defined FCC structure. Further evidence for the biosynthesis of Ag-NPs is provided by the presence of well-defined bands in the Bragg peaks of the XRD pattern, which correspond to crystalline Ag-NPs. The presence of reducing agents during the reaction likely stabilized the Ag-NPs, which led to the formation of the observed crystalline structure.

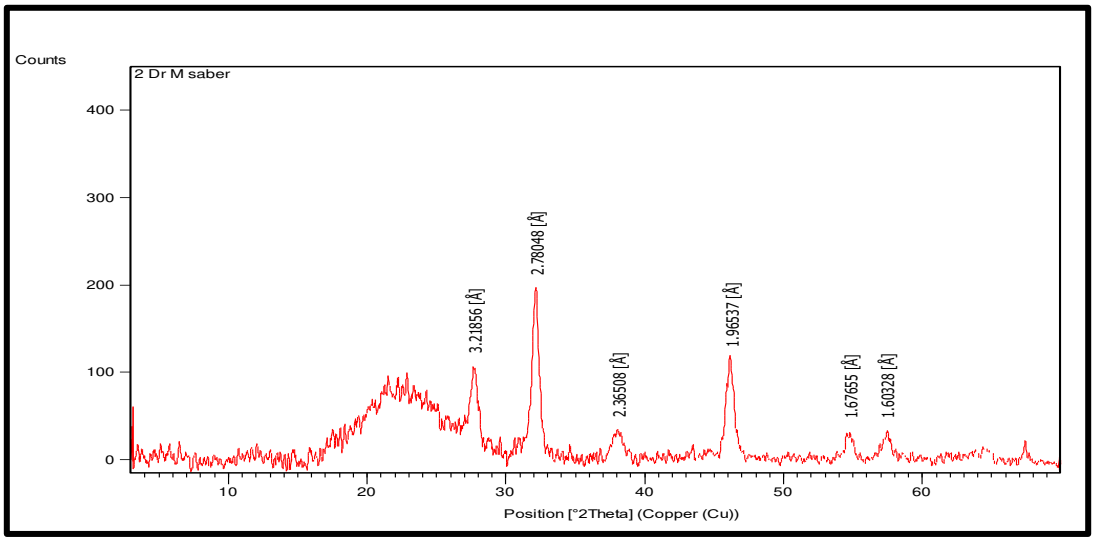

Figure 3. XRD Analysis Pattern of (Ag-NPs) Synthesized by Fungal Isolate (MK4).

3.5. Analysis via Transmission Electron Microscopy (TEM)

As shown in Figure 4, the TEM observation provided conclusive proof of the production of monocrystalline silver particles. The average particle size of the Ag-NPs was 15 ± 0.8 nm, and their shape was mostly spherical, with uniform diameters. While a few instances of larger-sized particles were identified in the sample, their overall quantity was considerably lower.

Preprints (www.preprints.org) | NOT PEER-REVIEWED | Posted: 26 December 2023 doi:10.20944/preprints202312.1737.v1

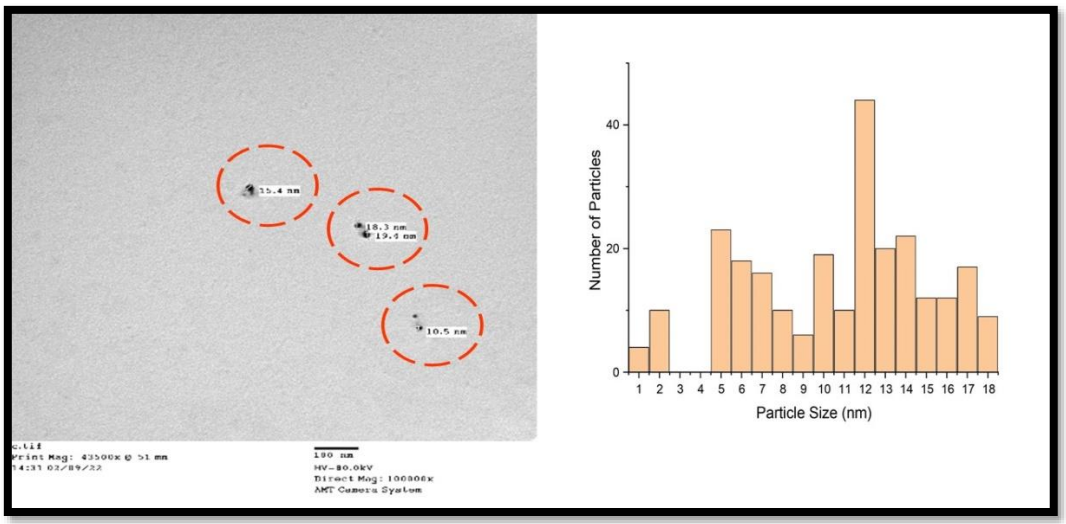

Figure 4. The use of a transmission electron microscope (TEM) for production of silver nanoparticles.

3.6. Sequencing the most effective fungal isolate (MK4)

During the detection phase, the most effective marine fungal isolate (MK4), which is capable of producing silver nanoparticles, was chosen. Phenotypic and molecular phylogenetic studies were both used in the classification process. Fungal isolate MK4 was used to extract genomic DNA, which was then partially amplified of the 18S rRNA gene. The resulting amplicons were visualized through agarose gel electrophoresis. There was a perfect match between the 18S rRNA gene sequence and *Aspergillus flavus*. The *Aspergillus flavus* MK4 nucleotide sequence is stored in the GenBank database underneath the accession number OQ651270. Figure 5 illustrates the phylogenetic relationships between the experimental strains and their most closely related species.

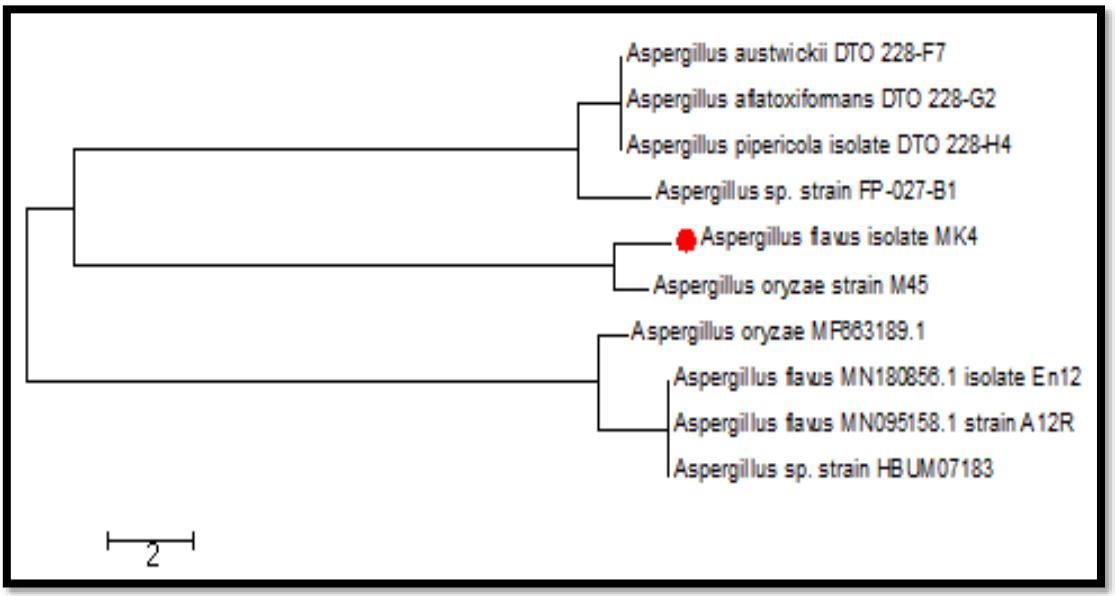

Figure 5. Phylogenetic analysis of *Aspergillus flavus* MK4 based on partial sequencing of 18S rDNA.

3.7. Antibacterial activity

Seven pathogenic bacteria, three of which were gram-positive and four of which were gram-negative, were tested for their antibacterial efficacy using the porous well diffusion technique in this study. Each well received 60 microliters of Ag nanoparticles solution, 1 mM silver nitrate, culture broth (without $AgNo_3$) as a negative control, and ampicillin (1 mg/ml) as a positive control. The in

Preprints (www.preprints.org) | NOT PEER-REVIEWED | Posted: 26 December 2023 doi:10.20944/preprints202312.1737.v1

vitro antibacterial activity of *Aspergillus flavus* MK4 was conducted and detailed in Table 1. The study proved that silver nanoparticles inhibited a wide range of gram-positive and gram-negative bacteria, demonstrating their broad-spectrum antibacterial activity. The results suggest the presence of antibacterial compounds in the nanoparticles that could be explored for treating illnesses caused by these microorganisms. *Staphylococcus aureus* ATCC 25923 and *Pseudomonas fluorescens* DSM 50090 had the largest inhibitory zones (average diameter: 30 mm) among the strains that were examined, whereas *Salmonella typhimurium* ATCC 14028 and *Aeromonas hydrophila* NRRL 914 had the smallest.

Table 1. Antimicrobial efficacy of silver nanoparticles on pathogenic microorganisms.

Pathogenic organism	CF	$AgNo_3$	Ag-NPs	Ampicillin (1 mg/ml)
Bacillus subtillus ATCC 6633	0.0	10 ± 0.01^a	28 ± 0.25^b	44 ± 0.01^a
Staphylococcus aureus ATCC 25923	0.0	6 ± 0.21^b	30 ± 0.2^a	40 ± 0.01^a
Bacillus cereus	0.0	6 ± 0.01^a	26 ± 0.01^b	40 ± 0.01^a
Pseudomonas aeruginosa ATCC 9027	0.0	8 ± 0.5^a	22 ± 0.2^b	40 ± 0.01^a
Salmonella typhimurium ATCC 14028	0.0	6 ± 0.02^a	14 ± 0.1^a	42 ± 0.01^a
Pseudomonas fluorescens DSM 50090	0.0	12 ± 0.1^a	30 ± 0.05^a	40 ± 0.01^a
Aeromonas hydrophila NRRL 914	0.0	4 ± 0.1^a	14 ± 0.2^a	40 ± 0.01^a

* (CF): Culture filtrate, ($AgNo_3$): Silver nitrate, (Ag-NPs): Silver nanoparticles, Means a-d with different superscripts in the same row are deemed significantly different (LSD test, $P < 0.05$), and triplicate measurements from two separate experiments were averaged with ±SD.

3.8. Anti-Fungal activity

By employing the time-tested agar well diffusion method, the research tested the antifungal effectiveness of biosynthesized Ag-NPs against several fungus strains. Table 2 indicated that the Ag-NPs were highly effective against all of the tested fungus, suggesting that they could be useful as antifungal agents. Ag-NPs had the capability to prevent fungal proliferation in *Aspergillus fumigatus*, *Aspergillus niger*, *Aspergillus flavus*, *Aspergillus terreus*, *Aspergillus parasiticus*, *Penicillium oxalicum*, *Fusarium solani*, *Fusarium oxysporum*, and *Candida albicans* where the areas of inhibition were 16 ± 0.12, 22 ± 0.1, 20 ± 0.02, 18 ± 0.01, 16 ± 0.02, 14 ± 0.04, 16 ± 0.1, 20 ± 0.1 and 18 ± 0.2 mm, respectively. The effect of $AgNO_3$ on fungi was limited, and additionally, no impact of nystatin was observed on any type of pathogenic fungi.

Table 2. Inhibition zones of Ag-NPs against selected fungal isolates.

Pathogenic fungi	$AgNo_3$	Ag-NPs	Nystatin
A. fumigatus (NIOF-F3)	8 ± 0.01^a	16 ± 0.12^b	0.0
A. niger (NIOF-F8)	4 ± 0.21^b	22 ± 0.1^a	0.0
A. flavus (NIOF-F12)	0.0	20 ± 0.02^b	0.0
A. terreus (NIOF-F13)	0.0	18 ± 0.01^b	0.0
A. parasiticus (NIOF-F15)	8 ± 0.02^a	16 ± 0.02^b	0.0
P. oxalicum (NIOF-F22)	10 ± 0.1^a	14 ± 0.04^a	0.0
F. solani (NIOF-F48)	4 ± 0.1^b	16 ± 0.1^b	0.0
F. oxysporum (NIOF-F63)	6 ± 0.1^a	20 ± 0.1^a	0.0
C. albicans (NIOF-F71)	10 ± 0.1^a	18 ± 0.2^a	0.0

* Silver nitrate, (Ag-NPs): Silver nanoparticles, Means a-d with different superscripts in the same row are deemed significantly different (LSD test, $P < 0.05$), and triplicate measurements from two separate experiments were averaged with ±SD.

 doi:10.20944/preprints202312.1737.v1

3.9. Antioxidant activity

The results indicated that both vitamin C and Ag-NPs could function as antioxidants. Specifically, Ag-NPs exhibited an antioxidant activity of 47.5%, surpassing the 29.4% antioxidant activity observed with vitamin C (refer to Figure 6). These findings highlight the significantly superior antioxidant activity of Ag-NPs compared to vitamin C.

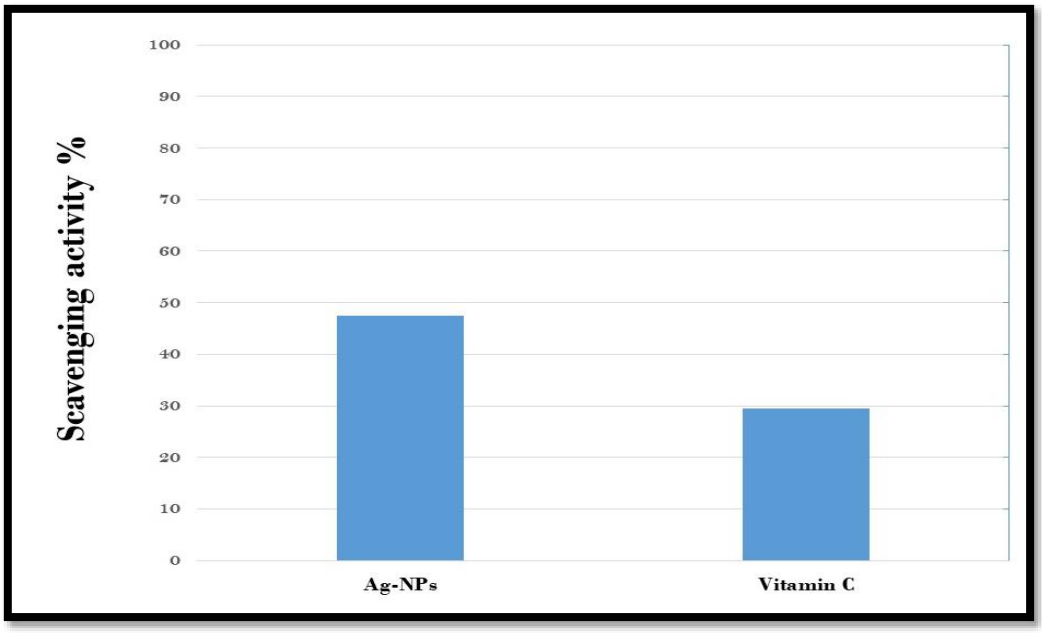

Figure 6. Comparison of the antioxidant activity (%) of produced silver nanoparticles with the conventional vitamin C.

3.10. Cytotoxic activity against human liver cancer cell (HepG-2)

The silver nanoparticles synthesized through biological means were utilized in a cytotoxicity study against the HepG-2 cell line to investigate their potential for the development of anti-cancer medications. The MTT assay was utilized to assess the percentage of viable HepG-2 cells following exposure to the biosynthesized silver nanoparticles at different concentrations. Figure 7 illustrates the varying percentages of viable cells under different Ag-NP concentrations. Notably, silver nanoparticles derived from *Aspergillus flavus* MK4 demonstrated a considerable level of anticancer activity, with determined IC_{50} values of 34.12 ± 1.05 (µg/Well) after a 24-hour exposure.

Preprints (www.preprints.org) | NOT PEER-REVIEWED | Posted: 26 December 2023 doi:10.20944/preprints202312.1737.v1

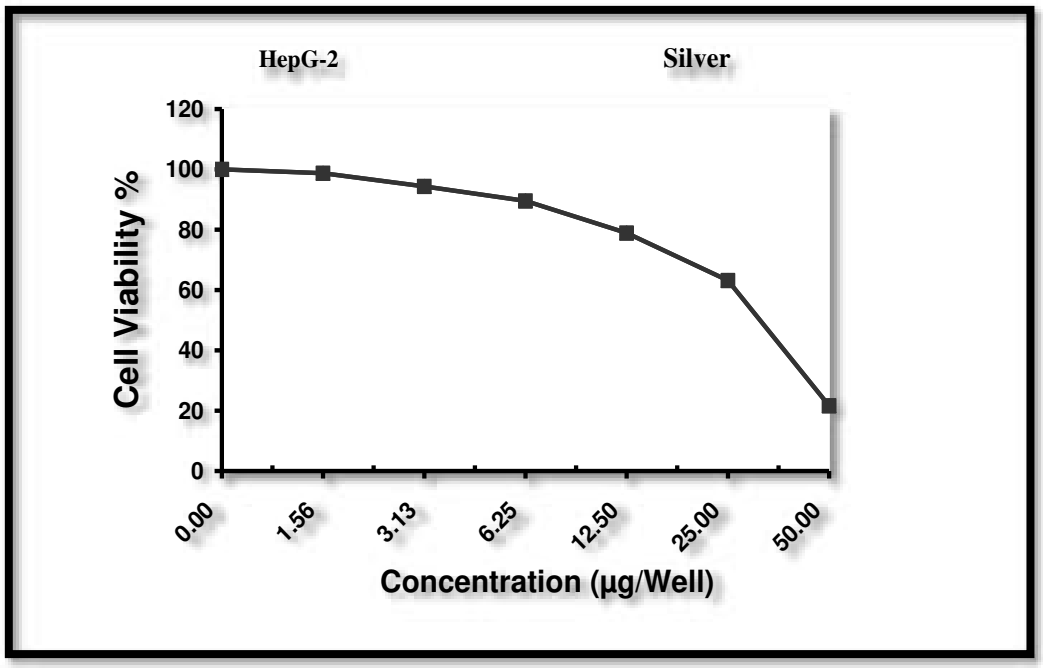

Figure 7. The IC50 value of HepG2 cells was determined after a 24-hour exposure to escalating dosages of (Ag-NPs) generated by Aspergillus *flavus* MK4.

3.11. Wound Healing Assay

The investigation revealed that silver nanoparticles contributed to accelerated wound healing, as depicted in Figures 8A–B. The proliferation of 3T3 fibroblast cells was monitored using the in vitro wound scratch method, capturing images of the scratched area at regular intervals to observe the impact of biogenic Ag-NPs. The concentration of Ag-NPs was quantified using the MTT test, with a concentration of 25 µg/ml Ag-NP applied, which is below the IC_{50} value. The healing of scar tissue occurred following Ag-NP treatment due to the activation of fibroblasts and cell migration. Remarkably, after 72 hours, the scar on the Ag-NP-treated plates had completely healed, mirroring the healing observed in the control group.

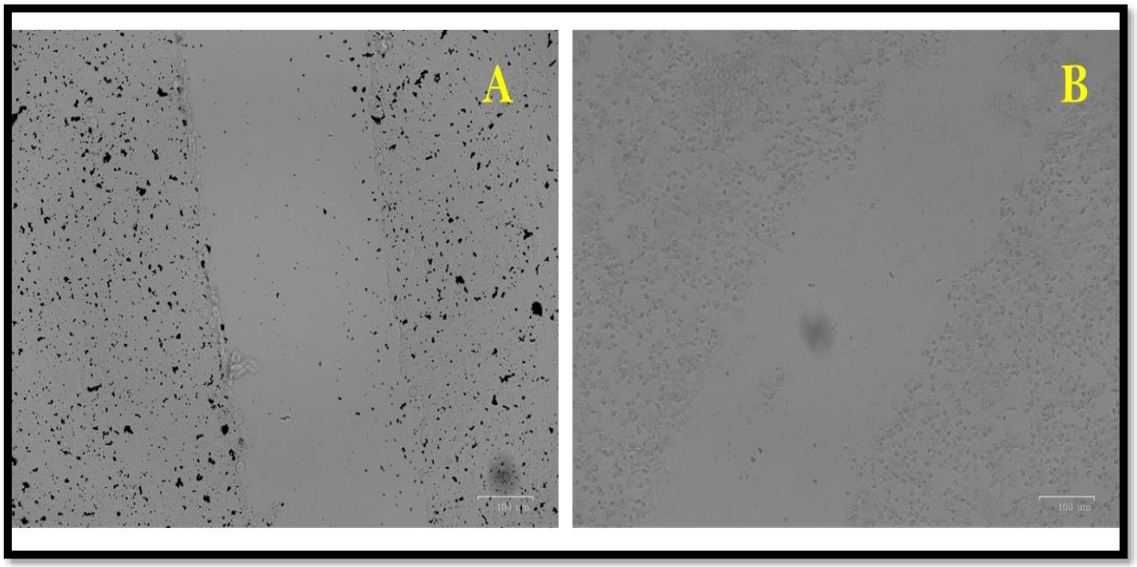

Figure 8. (A) 3T3 cells before being treated with silver nanoparticles, **(B)** 3T3 cells treated with silver nanoparticles. .

4. Discussion

 doi:10.20944/preprints202312.1737.v1

Nanotechnology has recently developed into an interdisciplinary area, incorporating ideas and research from many other scientific and medical fields, as such as mathematics, engineering, biology, materials science, physics, and chemistry [24]. A broad range of materials can be converted into nanoparticles by physical, chemical, and biological interactions. Biological methods for creating nanoparticles are the most encouraging of these technologies. [25]. This study delves deeper into the realm of nanoparticle synthesis by focusing on the biological approach utilizing marine fungi specifically isolated from Egypt's Red Sea. This method holds significant advantages, eliminating the need for potentially harmful chemicals, extreme temperatures, or high pressures. This inherent simplicity translates to a straightforward and scalable process, paving the way for potential large-scale production [26]. Fungi demonstrate significant potential for the production of a wide array of chemicals with diverse applications. Ascomycetes, imperfect fungi, and other microscopic filamentous fungi contribute to the creation of approximately 6,400 bioactive compounds [27]. Their capacity to absorb and bio-accumulate heavy metals make them ideal reducing and stabilizing agents, and these organisms are often used for this purpose. Fungi, being amenable to large-scale cultivation, are also well-suited to serve as "nano factories," facilitating the generation of nanoparticles with precisely manipulated size and shape [28]. The generation of Ag-NPs was achieved in this investigation by reducing aqueous Ag+ with the culture supernatants of marine fungal isolates at 28 ± 2°C. The brownish hue of the water-based solution, caused by both surface plasmon resonances (SPR) and the reduction of AgNO3, served as an obvious indicator of the synthesis of Ag-NPs [29]. As soon as the AgNO3 solution was added to the crude cell filtrate of the isolate MK4, the color changed from yellow to dark brown. The culture supernatant devoid of AgNO3 underwent no such alteration, as shown in Figure 1. The clear change in color signified the obvious creation of Ag-NPs. Even after 24 hours of incubation, the color intensity of the cell filtrate containing AgNO3 remained consistent, suggesting that the particles were evenly distributed in the solution [27]. Fungi possess an advantage over other microorganisms due to their prolific production of proteins and enzymes. This attribute enables fungi to synthesize nanoparticles quickly and sustainably, making them a favorable choice for nanoparticle production [30]. Although several studies have focused on the biogenic manufacture of silver nanoparticles utilizing fungus, our understanding of the underlying mechanisms is still limited. Enzymes found in fungal filtrate catalyze the extracellular creation of nanoparticles, which involves the conversion of silver ions to elemental silver (Ag0) at the nano-scale. Impact of that reaction on the material's optical properties is evident through surface plasmon resonance bands, observable with UV-visible spectroscopy in the newly colored filtrate after the reaction. When silver nitrate solutions were exposed to the isolate MK4, a noticeable color shift occurred, indicating the presence of UV-visible spectra associated with production of nanoparticles. The characteristic absorption band linked to surface plasmon was observed at 460 nm, as depicted in Figure 1. Absorbance peaks at longer wavelengths suggest the existence of larger nanoparticles, with the wavelength range of these bands spanning from 400 to 460 nm [31]. A noticeable peak at 440 nm, which is the surface plasmon resonance band, was observed in the UV-visible spectra of the cell filtrate produced by Aspergillus terreus with AgNO3. Based on these findings, it is highly probable that the solution contained (Ag-NPs) [29]. A peak at 420 nm was seen in the UV-visible spectra of silver nanoparticles synthesized using the fungus *T. harzianum* and *T. viride*. For *T. viride* and *T. harzianum* generated silver nanoparticles, respectively, the peak indicates the highest plasmon absorption. [32]. Using Fourier Transform-Infrared Spectroscopy (FT-IR) to examine protein-Ag-NP interactions demonstrated that biomolecules were pivotal in lowering silver ion concentrations and stabilizing Ag-NPs amounts in the solution. The cell-free extract, comprising biomolecules such as peptides, proteins, and carbohydrates, was analyzed within the range of 400–4000 cm^{-1} at a resolution of 4 cm^{-1}. Figure 2 demonstrated how primary amine (N-H) stretching was indicated by a clearly visible amine vibration band at 3417.58 cm-1. Furthermore, aromatic and aliphatic amine C-N stretching vibrations were characterized by two bands at 1383.59 and 1023.85 cm-1, respectively. This work provided irrefutable evidence that proteins play a crucial role in maintaining the stability of the silver nanoparticles synthesized from the cell-free filtrate of the selected isolate. Protein molecules released from outside the cell likely helped with the synthesis and

 doi:10.20944/preprints202312.1737.v1

stability of silver nanoparticles [33]. The FTIR spectral examination of the microbial filtrate subjected to silver nitrate identified functional groups, which could have formed between amino acid residues and proteins produced during the creation of the silver nanoparticles. By identifying peaks linked to particular functional groups, the research probably shed light on how biomolecules interacted with the silver nanoparticles throughout production [34]. Proteins play a crucial role in ensuring the stability of the generated nanoparticles; the FTIR spectra show peaks at 1629 and 1356 cm-1, confirming their presence. In proteins, the bands often represent the stretching of C-C and C-N bonds, respectively. This finding provides more evidence that proteins play a role in the process that stabilizes the silver nanoparticles that are created [35]. We used XRD and TEM to analyze the produced Ag-NPs in depth, hoping to uncover new applications for them. The crystalline characteristics of Ag-NPs were examined in this study using X-ray diffraction (XRD). Six diffraction peaks were seen at 2θ values of 28.8°, 32.7°, 37.9°, 45.0°, 55.4°, and 58.4°, respectively, representing the (111), (200), (024), (311), (116), and (222) lattice planes, as shown in Figure 3. These peaks align with the silver cubic structure's standard diffraction pattern, indicating a high-quality crystal structure for the Ag-NPs. Specifically, the presence of the (111) planes, characterized by the peak at 28.8°, is typical for silver metal crystals. The cubic crystal structure, evident in the unit cell's appearance, further confirms the quality of the Ag-NPs. To gain deeper insights into the structure and morphology of the Ag-NPs, TEM analysis was conducted. Figure 4 shows electromagnetic transmission illustrations that show the particles are of the same size and shape, and they are not clumped together. Particle sizes of the Ag-NPs varied between 2 and 18 nm. According to San and Don's [36] study on the green synthesis of Ag-NPs with the white rot fungus P. sanguineus, the resulting particles are spherical, polydisperse, and have a size range of 1 to 20 nm, as shown in transmission electron microscopy (TEM) images. The average size of the silver particles produced by Aspergillus terreus ranged from 8 to 20 nm, according to a size distribution analysis that measured the diameters of 120 silver nanoparticles randomly selected in TEM images [37]. As per Ammar and El-Desouky's investigation, the dimensions of Ag-NPs ranged from 14 to 25 nm in the case of *P. expansum* and between 10 and 18 nm for *A. terreus* [38]. The comprehensive molecular investigations, coupled with classical taxonomy outcomes, robustly affirmed the categorization of the isolated strain as *Aspergillus flavus*. You may find the nucleotide sequence in the Genome library with the code **OQ651270**. Figure 5 illustrates the phylogenetic connections among the representative experimental strains and their closest species counterparts. The capacity of *Aspergillus* spp. to quickly produce stable particles makes them an attractive strain for the extracellular manufacture of metal nanoparticles, according to this research. *Aspergillus* spp. have been repeatedly named as strong candidates for silver nanoparticle synthesis in a plethora of investigations [39-44]. In general, the silver nanoparticles (Ag-NPs) exhibited effective inhibition against a range of bacterial species, albeit with varying degrees of efficacy. Contrary to the antibacterial impact being contingent on the Gram classification (positive or negative), our research findings indicate that the effectiveness of Ag-NPs is more closely tied to the specific bacterial species. This variability is likely attributed to the distinct membranes and cell walls inherent in different bacterial species. While screening against various bacteria, the most potent effects were seen against *Staphylococcus aureus* and *Proteus mirabilis*, with *B. subtilis* coming in third. The antibacterial activities of Ag-NPs were more strongly resisted by *S. typhimurium* and *A. hydrophila* than by any of the other bacterial species. Size has a significant impact on the effectiveness of silver nanoparticles in suppressing bacteria [33, 36]. More evidence that the antibacterial effectiveness of nanoparticles depends on their particular forms has come from studies that looked at how different shaped nanoparticles inhibited bacterial growth. The influence of silver nanoparticles on bacterial cells is determined to be contingent on their shape, resulting in diverse outcomes depending on the morphologies of the nanoparticles. According to a number of studies, silver nanoparticles (Ag-NPs) can impede cellular respiration by adhering to cell membrane surfaces, which can disrupt membrane permeability. The greater surface area of smaller silver nanoparticles makes them more effective in killing bacteria than bigger nanoparticles [45]. It is possible that (Ag-NPs) could penetrate bacterial cells via interacting with their membrane. Because of their size, surface characteristics, and other unique qualities, Ag-NPs may interact with bacterial membranes, changing

 doi:10.20944/preprints202312.1737.v1

their permeability and integrity. Nanoparticles may be able to enter the bacterial cell more easily if this interaction disrupts the membrane structure. Upon entering the cell, silver nanoparticles can exert their antibacterial properties by diverse ways, including disrupting cellular processes, producing oxidative stress, or interacting with vital biomolecules. The precise mechanisms of action can differ based on factors like the size, shape, and surface chemistry of the nanoparticles, in addition to the distinct characteristics of the bacterial species in question [46]. The enormous surface area of silver nanoparticles, in comparison to other salts, is undoubtedly responsible for their strong antibacterial action. The augmented surface area offers greater possibilities for interaction and contact with microbiological organisms. This improved contact enables a stronger influence on the microbial cell membranes and internal structures, resulting in increased antibacterial effectiveness. The exceptional antibacterial efficacy of silver nanoparticles can be attributed mostly to their unique physicochemical characteristics, such as their dimensions, morphology, and surface properties. Due to their capacity to engage extensively with microbial surfaces and potentially infiltrate cells, they exhibit effectiveness in altering bacterial structures and functions. The significant ratio of surface area to volume is a crucial determinant that distinguishes silver nanoparticles from other salts in relation to their antibacterial characteristics [47]. The nanoparticles have the capacity to both penetrate the bacterium and form a bond with the cell membrane. Silver nanoparticles demonstrate a strong attraction to phosphorus-containing molecules, such as DNA, as well as proteins that include sulfur, which are present in bacterial membranes. Upon entry of silver nanoparticles into the bacterium, a localized region of reduced molecular weight becomes evident within the cell. The bacteria congregate here to shield the DNA from the ions of silver. Nanoparticles cause cell division and, eventually, cell death by targeting the respiratory chain. Because silver ions are released intracellularly, the nanoparticles have enhanced bactericidal activity [48]. Unlike Gram-positive bacteria, which possess a denser peptidoglycan layer impeding the entry of Ag-NPs into their cells, research indicates that Ag-NPs exhibit heightened toxicity towards Gram-negative bacteria. This increased toxicity is attributed to Ag-NPs easily penetrating the thinner outer membrane of Gram-negative bacteria and causing damage to their proteins and DNA. A greater concentration of Ag-NPs is necessary to cause death in Gram-positive bacteria because their peptidoglycan covering is thicker [49]. The subsequent zones of inhibition were reported in the research conducted by Narasimha and his team on the antibacterial capabilities of (Ag-NPs) generated from mushrooms: Bacillus sp., 1.9 cm, E. coli, P. aeruginosa, and S. aureus all fall into this range. Particles with a larger contact surface area, such as those between 10 and 20 nm in size, are more efficient against both gram-positive and gram-negative bacteria, according to the study's authors [50]. Similarly, at a concentration of 100 µg mL−1, the silver nanoparticles (Ag-NPs) made from the water-based extract of *Aspergillus flavus* showed significant antibacterial and antifungal effects against various microorganisms, including *S. aureus*, *B. subtilis*, *P. aeruginosa*, *E. coli*, *Candida albicans*, *Candida glabrata*, *Candida tropicalis* and *Candida parapsilosis* [51]. Fouda and his team's findings indicate that the application of (Ag-NPs) produced by *P. italicum* resulted in clear areas of suppression for different microbes. Specifically, treatment with these Ag-NPs resulted in clear zones measuring 17.6 ± 2.2 mm for *S. aureus*, 19.5 ± 0.5 mm for *E. coli*, 35.0 ± 0.5 mm for *C. albicans*, and 35.6 ± 0.6 mm for *C. tropicalis*, all observed at a concentration of 100 ppm [51]. The results of the effectively dispersion technique showed that Ag-NPs inhibited the growth of the tested strains of fungi, including *A. fumigatus* (NIOF-F3), *A. niger* (NIOF-F8), *A. flavus* (NIOF-F12), *A. terreus* (NIOF-F13), *A. parasiticus* (NIOF-F15), *P. oxalicum* (NIOF-F22), *F. solani* (NIOF-F48), *F. oxysporum* (NIOF-F63), and *Candida albicans* (NIOF-F71). The data presented in Table 2 demonstrates that *Aspergillus niger* exhibited higher susceptibility to Ag-NPs compared to other fungal isolates, displaying an inhibition zone of approximately 22 ± 0.1 mm with an optimal volume of 60 µl of the as-prepared Ag-NPs solution. Antifungal properties of metallic nanoparticles have recently attracted attention [52, 53]. These nanoparticles include silver, zinc, copper, titanium, and others. The anticandidal activity of silver nanoparticles (Ag-NPs) biosynthesized by endophytic *Rothia endophytica* against *Candida albicans* was noted by Elbahnasawy et al. [54]. Ajaz et al. [55] tested ZV-Ag-NPs against the common plant disease *Colletotrichum falcatum* to see how effective they were as an antifungal. In vitro comparisons between the fungal mycelia and the control group revealed a

significant inhibitory impact of ZV-Ag-NPs at a dosage of 20 µg/mL. Irrespective of the mycotoxigenic fungi *A. flavus* and *A. ochraceus*, Ag-NPs synthesized from cell-free culture filtrates of *Penicillium chrysogenum* and *F. chlamydosporum* showed significant antifungal efficacy [56]. At a dosage of 100 µg/mL, biogenic silver nanoparticles produced by *Syzygium cumini* leaf extract show antifungal action against *A. flavus* and *A. parasiticus* strains of fungus [57]. The antioxidant properties of silver nanoparticles are attributed to the adsorption of fungal components from a cell-free filtrate onto the nanoparticles [58]. As depicted in Figure 7, the (Ag-NPs) exhibited an antioxidant activity of approximately 47.5%, surpassing the antioxidant activity of vitamin C, which was approximately 29.4%. The findings indicate that the antioxidant potential of Ag-NPs exceeds that of vitamin C. Marine fungi, characterized by diverse biological traits such as antioxidant, antibacterial, and antimalarial activities, are proficient in producing metal nanoparticles. Here, the seaweed-isolated marine endophytic fungus *C. cladosporioides* has produced silver nanoparticles that are rich in antioxidants [19]. This discovery offers compelling evidence supporting the effective use of silver nanoparticles as natural antioxidants, capable of providing protection against oxidative stressors and degenerative diseases with which they are associated [59]. Biogenic silver nanoparticles demonstrate impacts on tumor cells that extend beyond their widely recognized antibacterial properties [27]. Figure 8 shows that the viability of a tumor cell line is reduced by silver nanoparticles in a dose-dependent manner. More specifically, the HepG-2 cell line was shown to be resistant to the anticancer effects of silver nanoparticles produced by *Aspergillus flavus* MK4. Researchers Husseiny and colleagues attempted to determine whether silver nanoparticles produced by *Fusarium oxysporum* had any antibacterial or anticancer effects. The effectiveness of these nanoparticles against *E. coli* and *S. aureus* was further demonstrated by their ability to limit the growth of a tumor cell line. The nanoparticles showed great cytotoxicity and the possibility of efficient tumor control when they were exposed to MCF-7 cells, as evidenced by a low IC50 value of 121.23 µg/cm3 [60]. Silver nanoparticles produced by fungi demonstrated robust anticancer activity against various tumor cell lines, exhibiting IC_{50} values that align with those reported in prior studies [39, 41, 61-64]. In Figures 8A-B, we can see the results demonstrating that silver nanoparticles accelerate the healing process of wounds. Silver nanoparticles' potential as a medicinal agent is enhanced by their shown ability to repair wounds. The medicinal uses of silver nanoparticles in promoting skin regeneration and wound healing have been previously documented [65-68]. Hence, the current study's discovery indicating the promising wound-healing potential of silver nanoparticles derived from a fungal extract holds great promise for biomedical applications.

5. Conclusions

The X-ray dispersion, UV-Vis spectroscopy, transmission electron microscopy, and Fourier transform infrared spectroscopy were used to characterize the successfully synthesized silver nanoparticles that were made from the marine fungal strain Aspergillus flavus MK4. The nanoparticles that were created exhibited a surface plasmon resonance at 460 nm, and a TEM analysis revealed that there were silver nanoparticles measuring 15 nm in size. The agar well diffusion assay was utilized to evaluate the antibacterial characteristics of the produced silver nanoparticles against bacterial and fungal pathogens. The assessment proved that the nanoparticles are antimicrobially effective. Moreover, the study highlights the availability and potential biomedical applications of Ag-NPs, including anticancer and wound healing properties, which make them attractive for further exploration in various catalytic and medical uses. The investigation emphasizes cost-effectiveness in cultivation requirements and rapid development in the laboratory, all while being environmentally friendly. The results confirm that the micron-sized particles have been effectively produced and highlight how effective and powerful the antibacterial properties of silver nanoparticles are.

Acknowledgments: The authors are thankful to the Researchers Supporting Project number (RSP2024R516) at King Saud University, Riyadh, Saudi Arabia.

References

1. Grossart H-P, Van den Wyngaert S, Kagami M, Wurzbacher C, Cunliffe M, Rojas-Jimenez K: **Fungi in aquatic ecosystems**. *Nature Reviews Microbiology* 2019, **17**(6):339-354.
2. Hyde KD, Jeewon R, Chen Y-J, Bhunjun CS, Calabon MS, Jiang H-B, Lin C-G, Norphanphoun C, Sysouphanthong P, Pem D: **The numbers of fungi: is the descriptive curve flattening?** *Fungal Diversity* 2020, **103**:219-271.
3. Jayasiri SC, Hyde KD, Ariyawansa HA, Bhat J, Buyck B, Cai L, Dai Y-C, Abd-Elsalam KA, Ertz D, Hidayat I: **The Faces of Fungi database: fungal names linked with morphology, phylogeny and human impacts**. *Fungal diversity* 2015, **74**:3-18.
4. Deshmukh SK, Prakash V, Ranjan N: **Marine fungi: A source of potential anticancer compounds**. *Frontiers in microbiology* 2018, **8**:2536.
5. Lal HM, Thomas S, Li T, Maria HJ: Polymer Nanocomposites Based on Silver Nanoparticles: Springer; 2021.
6. Dikshit PK, Kumar J, Das AK, Sadhu S, Sharma S, Singh S, Gupta PK, Kim BS: **Green synthesis of metallic nanoparticles: Applications and limitations**. *Catalysts* 2021, **11**(8):902.
7. De Silva C, Nawawi NM, Abd Karim MM, Abd Gani S, Masarudin MJ, Gunasekaran B, Ahmad SA: The mechanistic action of biosynthesised silver nanoparticles and its application in aquaculture and livestock industries. *Animals* 2021, 11(7):2097.
8. Xu L, Yi-Yi W, Huang J, Chun-Yuan C, Zhen-Xing W, Xie H: **Silver nanoparticles: Synthesis, medical applications and biosafety**. *Theranostics* 2020, **10**(20):8996.
9. Bamal D, Singh A, Chaudhary G, Kumar M, Singh M, Rani N, Mundlia P, Sehrawat AR: Silver nanoparticles biosynthesis, characterization, antimicrobial activities, applications, cytotoxicity and safety issues: An updated review. *Nanomaterials* 2021, 11(8):2086.
10. Mistry H, Thakor R, Patil C, Trivedi J, Bariya H: Biogenically proficient synthesis and characterization of silver nanoparticles employing marine procured fungi Aspergillus brunneoviolaceus along with their antibacterial and antioxidative potency. *Biotechnology Letters* 2021, 43:307-316.
11. Nasrollahzadeh M, Sajadi SM, Issaabadi Z, Sajjadi M: **Biological sources used in green nanotechnology**. In: *Interface science and technology*. vol. 28: Elsevier; 2019: 81-111.
12. Abdel-Hameed SM, Abd Allah NA, Hamed MM, Soltan OI: **Papaya fruit by-products as novel food ingredients in cupcakes**. *Annals of Agricultural Sciences* 2023, **68**(1):60-74.
13. Gaddeyya G, Niharika PS, Bharathi P, Kumar PR: **Isolation and identification of soil mycoflora in different crop fields at Salur Mandal**. *Advances in Applied Science Research* 2012, **3**(4):2020-2026.
14. Alsohaili SA, Bani-Hasan BM: Morphological and molecular identification of fungi isolated from different environmental sources in the Northern Eastern desert of Jordan. *Jordan Journal of Biological Sciences* 2018, 11(3).
15. Pallavi S, Rudayni HA, Bepari A, Niazi SK, Nayaka S: Green synthesis of Silver nanoparticles using Streptomyces hirsutus strain SNPGA-8 and their characterization, antimicrobial activity, and anticancer activity against human lung carcinoma cell line A549. *Saudi Journal of Biological Sciences* 2022, 29(1):228-238.
16. Verma VC, Kharwar RN, Gange AC: Biosynthesis of antimicrobial silver nanoparticles by the endophytic fungus Aspergillus clavatus. *Nanomedicine* 2010, 5(1):33-40.
17. Mistry H, Thakor R, Patil C, Trivedi J, Bariya H: Biogenically proficient synthesis and characterization of silver nanoparticles employing marine procured fungi Aspergillus brunneoviolaceus along with their antibacterial and antioxidative potency. *Biotechnology Letters* 2021, 43(1):307-316.
18. Bao Z, Ikunaga Y, Matsushita Y, Morimoto S, Takada-Hoshino Y, Okada H, Oba H, Takemoto S, Niwa S, Ohigashi K: **Combined analyses of bacterial, fungal and nematode communities in andosolic agricultural soils in Japan**. *Microbes and environments* 2012, **27**(1):72-79.
19. Hulikere MM, Joshi CG: Characterization, antioxidant and antimicrobial activity of silver nanoparticles synthesized using marine endophytic fungus-Cladosporium cladosporioides. *Process biochemistry* 2019, 82:199-204.
20. Hashem AH, Khalil AMA, Reyad AM, Salem SS: Biomedical applications of mycosynthesized selenium nanoparticles using Penicillium expansum ATTC 36200. *Biological trace element research* 2021:1-11.
21. Hashem AH, Saied E, Amin BH, Alotibi FO, Al-Askar AA, Arishi AA, Elkady FM, Elbahnasawy MA: Antifungal activity of biosynthesized silver nanoparticles (AgNPs) against aspergilli causing aspergillosis: Ultrastructure Study. *Journal of Functional Biomaterials* 2022, 13(4):242.
22. Nayak D, Ashe S, Rauta PR, Kumari M, Nayak B: Bark extract mediated green synthesis of silver nanoparticles: evaluation of antimicrobial activity and antiproliferative response against osteosarcoma. *Materials Science and Engineering: C* 2016, 58:44-52.
23. Mohanta YK, Panda SK, Jayabalan R, Sharma N, Bastia AK, Mohanta TK: Antimicrobial, antioxidant and cytotoxic activity of silver nanoparticles synthesized by leaf extract of Erythrina suberosa (Roxb.). *Frontiers in molecular biosciences* 2017, 4:14.
24. Rahman S, Rahman L, Khalil AT, Ali N, Zia D, Ali M, Shinwari ZK: **Endophyte-mediated synthesis of silver nanoparticles and their biological applications**. *Applied microbiology and biotechnology* 2019, **103**:2551-2569.

25. Gezaf SA, Hamedo HA, Ibrahim AA, Mossa MI: Mycosynthesis of silver nanoparticles by endophytic Fungi: Mechanism, characterization techniques and their applications. *Microbial Biosystems* 2022, 7(2):48-65.
26. Sandhu SS, Shukla H, Shukla S: Biosynthesis of silver nanoparticles by endophytic fungi: Its mechanism, characterization techniques and antimicrobial potential. *African Journal of Biotechnology* 2017, 16(14):683-698.
27. Guilger-Casagrande M, Lima Rd: **Synthesis of silver nanoparticles mediated by fungi: a review**. *Frontiers in bioengineering and biotechnology* 2019, **7**:287.
28. Khan N, Khan M, Jameel J, Jameel N, Rheman S: An overview: biological organisms that serves as nanofactories for metallic nanoparticles synthesis and fungi being the most appropriate. *Bioceram Dev Appl* 2017, 7(101):1-4.
29. Li G, He D, Qian Y, Guan B, Gao S, Cui Y, Yokoyama K, Wang L: **Fungus-mediated green synthesis of silver nanoparticles using Aspergillus terreus**. *International journal of molecular sciences* 2011, **13**(1):466-476.
30. Alghuthaymi MA, Almoammar H, Rai M, Said-Galiev E, Abd-Elsalam KA: **Myconanoparticles: synthesis and their role in phytopathogens management**. *Biotechnology & Biotechnological Equipment* 2015, **29**(2):221-236.
31. Rabab M, Raida E, Awatif A: Biosynthesis and characterization of silver nanoparticles using Trichoderm longibrachiatum and their effect on phytopathogenic fungi. *Egyptian Journal of Biological Pest Control* 2018, 28:28.
32. Elamawi RM, Al-Harbi RE, Hendi AA: Biosynthesis and characterization of silver nanoparticles using Trichoderma longibrachiatum and their effect on phytopathogenic fungi. *Egyptian journal of biological pest control* 2018, 28(1):1-11.
33. Gudikandula K, Vadapally P, Charya MS: Biogenic synthesis of silver nanoparticles from white rot fungi: Their characterization and antibacterial studies. *OpenNano* 2017, 2:64-78.
34. Nithya R, Ragunathan R: Synthesis of silver nanoparticles using a probiotic microbe and its antibacterial effect against multidrug resistant bacteria. *African Journal of Biotechnology* 2012, 11(49):11013-11021.
35. Nithya R, Ragunathan R: In vitro synthesis, characterization and medical application of silver nanoparticle by using a lower fungi. *Middle-East J Sci Res* 2014, 21(6):922-928.
36. San Chan Y, Don MM: Biosynthesis and structural characterization of Ag nanoparticles from white rot fungi. *Materials Science and Engineering: C* 2013, 33(1):282-288.
37. Balakumaran M, Ramachandran R, Balashanmugam P, Mukeshkumar D, Kalaichelvan P: Mycosynthesis of silver and gold nanoparticles: optimization, characterization and antimicrobial activity against human pathogens. *Microbiological research* 2016, 182:8-20.
38. Ammar H, El-Desouky T: Green synthesis of nanosilver particles by Aspergillus terreus HA1N and Penicillium expansum HA2N and its antifungal activity against mycotoxigenic fungi. *Journal of Applied Microbiology* 2016, 121(1):89-100.
39. Lotfy WA, Alkersh BM, Sabry SA, Ghozlan HA: Biosynthesis of silver nanoparticles by Aspergillus terreus: characterization, optimization, and biological activities. *Frontiers in bioengineering and biotechnology* 2021, 9:633468.
40. Rai R, Vishwanathan A, Vijayakumar B: Antibacterial Potential of Silver Nanoparticles Synthesized Using Aspergillus hortai. *BioNanoScience* 2023, 13(1):203-211.
41. Wang D, Xue B, Wang L, Zhang Y, Liu L, Zhou Y: Fungus-mediated green synthesis of nano-silver using Aspergillus sydowii and its antifungal/antiproliferative activities. *Scientific reports* 2021, 11(1):10356.
42. Gopa DR, Pullapukuri K: Green synthesis of silver nanoparticles from Aspergillus flavus and their antibacterial performance. *Chemical Product and Process Modeling* 2023.
43. Al-Zubaidi S, Al-Ayafi A, Abdelkader H: Biosynthesis, characterization and antifungal activity of silver nanoparticles by Aspergillus niger isolate. *Journal of Nanotechnology Research* 2019, 1(1):23-36.
44. Al-Soub A, Khleifat K, Al-Tarawneh A, Al-Limoun M, Alfarrayeh I, Al Sarayreh A, Al Qaisi Y, Qaralleh H, Alqaraleh M, Albashaireh A: **Silver nanoparticles biosynthesis using an airborne fungal isolate, Aspergillus flavus: optimization, characterization and antibacterial activity**. *Iranian Journal of Microbiology* 2022, **14**(4):518-528.
45. Bruna T, Maldonado-Bravo F, Jara P, Caro N: **Silver nanoparticles and their antibacterial applications**. *International Journal of Molecular Sciences* 2021, **22**(13):7202.
46. Morones JR, Elechiguerra JL, Camacho A, Holt K, Kouri JB, Ramírez JT, Yacaman MJ: **The bactericidal effect of silver nanoparticles**. *Nanotechnology* 2005, **16**(10):2346.
47. Logeswari P, Silambarasan S, Abraham J: Synthesis of silver nanoparticles using plants extract and analysis of their antimicrobial property. *Journal of Saudi Chemical Society* 2015, 19(3):311-317.
48. Silambarasan S, Abraham J: **Biosynthesis of silver nanoparticles**. *African Journal of Biotechnology* 2013, **12**(21).
49. Saravanan M, Arokiyaraj S, Lakshmi T, Pugazhendhi A: Synthesis of silver nanoparticles from Phenerochaete chrysosporium (MTCC-787) and their antibacterial activity against human pathogenic bacteria. *Microbial pathogenesis* 2018, 117:68-72.

50. Narasimha G, Praveen B, Mallikarjuna K, DEVA PRB: Mushrooms (Agaricus bisporus) mediated biosynthesis of sliver nanoparticles, characterization and their antimicrobial activity. 2011.
51. Fouda A, Awad MA, Al-Faifi ZE, Gad ME, Al-Khalaf AA, Yahya R, Hamza MF: Aspergillus flavus-mediated green synthesis of silver nanoparticles and evaluation of their antibacterial, anti-candida, acaricides, and photocatalytic activities. *Catalysts* 2022, 12(5):462.
52. Akpinar I, Unal M, Sar T: Potential antifungal effects of silver nanoparticles (AgNPs) of different sizes against phytopathogenic Fusarium oxysporum f. sp. radicis-lycopersici (FORL) strains. *SN Applied Sciences* 2021, 3(4):506.
53. Narware J, Yadav R, Keswani C, Singh S, Singh H: **Silver nanoparticle-based biopesticides for phytopathogens: Scope and potential in agriculture**. In: *Nano-biopesticides today and future perspectives.* Elsevier; 2019: 303-314.
54. Elbahnasawy MA, Shehabeldine AM, Khattab AM, Amin BH, Hashem AH: Green biosynthesis of silver nanoparticles using novel endophytic Rothia endophytica: Characterization and anticandidal activity. *Journal of Drug Delivery Science and Technology* 2021, 62:102401.
55. Ajaz S, Ahmed T, Shahid M, Noman M, Shah AA, Mehmood MA, Abbas A, Cheema AI, Iqbal MZ, Li B: Bioinspired green synthesis of silver nanoparticles by using a native Bacillus sp. strain AW1-2: Characterization and antifungal activity against Colletotrichum falcatum Went. *Enzyme and microbial technology* 2021, 144:109745.
56. Khalil NM, Abd El-Ghany MN, Rodríguez-Couto S: Antifungal and anti-mycotoxin efficacy of biogenic silver nanoparticles produced by Fusarium chlamydosporum and Penicillium chrysogenum at non-cytotoxic doses. *Chemosphere* 2019, 218:477-486.
57. Asghar MA, Zahir E, Asghar MA, Iqbal J, Rehman AA: Facile, one-pot biosynthesis and characterization of iron, copper and silver nanoparticles using Syzygium cumini leaf extract: as an effective antimicrobial and aflatoxin B1 adsorption agents. *PloS one* 2020, 15(7):e0234964.
58. Keshari AK, Srivastava R, Singh P, Yadav VB, Nath G: **Antioxidant and antibacterial activity of silver nanoparticles synthesized by Cestrum nocturnum**. *Journal of Ayurveda and integrative medicine* 2020, **11**(1):37-44.
59. Sulaiman GM, Hussien HT, Saleem MM: Biosynthesis of silver nanoparticles synthesized by Aspergillus flavus and their antioxidant, antimicrobial and cytotoxicity properties. *Bulletin of Materials Science* 2015, 38:639-644.
60. Garg H: An approach for solving constrained reliability-redundancy allocation problems using cuckoo search algorithm. *Beni-Suef University Journal of Basic and Applied Sciences* 2015, 4(1):14-25.
61. Chi NTL, Veeraragavan GR, Brindhadevi K, Chinnathambi A, Salmen SH, Alharbi SA, Krishnan R, Pugazhendhi A: **Fungi fabrication, characterization, and anticancer activity of silver nanoparticles using metals resistant Aspergillus niger**. *Environmental Research* 2022, **208**:112721.
62. Liu X, Chen J-L, Yang W-Y, Qian Y-C, Pan J-Y, Zhu C-N, Liu L, Ou W-B, Zhao H-X, Zhang D-P: **Biosynthesis of silver nanoparticles with antimicrobial and anticancer properties using two novel yeasts**. *Scientific Reports* 2021, **11**(1):1-12.
63. Kumari RM, Kumar V, Kumar M, Pareek N, Nimesh S: Assessment of antibacterial and anticancer capability of silver nanoparticles extracellularly biosynthesized using Aspergillus terreus. *Nano Express* 2020, 1(3):030011.
64. Waseem M, Nisar MA: **Fungal-derived nanoparticles as novel antimicrobial and anticancer agents**. In: *Functionalized Nanomaterials.* IntechOpen; 2016.
65. Al-saggaf MS: Formulation of insect chitosan stabilized silver nanoparticles with propolis extract as potent antimicrobial and wound healing composites. *International Journal of Polymer Science* 2021, 2021:1-9.
66. Paladini F, Pollini M: Antimicrobial silver nanoparticles for wound healing application: progress and future trends. *Materials* 2019, 12(16):2540.
67. Chinnasamy G, Chandrasekharan S, Koh TW, Bhatnagar S: Synthesis, characterization, antibacterial and wound healing efficacy of silver nanoparticles from Azadirachta indica. *Frontiers in microbiology* 2021, 12:611560.
68. Bold B-E, Urnukhsaikhan E, Mishig-Ochir T: Biosynthesis of silver nanoparticles with antibacterial, antioxidant, anti-inflammatory properties and their burn wound healing efficacy. *Frontiers in Chemistry* 2022, 10.